Journal of Thermal Analysis and Calorimetry, Vol. 75 (2004) 739–751

IN SITU PREPARED COMPOSITE OF ULTRAHIGH MOLECULAR MASS PE AND PANI
Thermal behavior and supramolecular structure

D. Tsocheva and L. Terlemezyan*

Institute of Polymers, Bulgarian Academy of Sciences, 1113 Sofia, Bulgaria

(Received February 18, 2003; in revised form October 7, 2003)

Abstract

Crystallinity parameters and changes in the crystalline morphology with temperature of an electrically conductive composite containing ultrahigh molecular mass polyethylene (UHMMPE) and polyaniline (PANI) doped with dodecylbenzenesulfonic acid (DBSA) are studied for the first time by using differential scanning calorimetry and wide-angle X-ray diffraction. It is found that during the melting of UHMMPE crystals PANI partially penetrates in the amorphous phase of the matrix polymer. Since the composite is found to be thermally stable up to ca. 270°C, it can be suggested that it would be processable without loosing conductivity at temperatures much higher than the melting temperature of UHMMPE.

Keywords: composite, crystallinity parameters, DSC, polyaniline, thermal stability, ultrahigh molecular mass polyethylene

Introduction

In the field of conductive polymers, polyaniline (PANI), in both doped and undoped state, has shown potential for large scale application due to its simple synthesis, good environmental stability and adequate levels of electrical conductivity [1, 2]. The commercial application of PANI, however, has been limited by its poor processability due to the rigid-rod macromolecular chains. Recent research on conducting PANI has targeted improving the flexibility and hence processability. Several methods have been developed to improve the processability by a postprocessing step, such as reprotonation of emeraldine base with a second protonic acid [3, 4] and functionalization of PANI emeraldine base [5, 6]. Efforts have also been focused on the use of surfactant to aid in processing of PANI derivatives [7, 8]. The replacement of inorganic acids, traditionally used in the doping process of PANI, by functionalized organic acids makes the polymer soluble in a series of organic solvents and enables the manufacture of conducting polymeric blends [9]. The use of, for example, dodecylbenzenesulfonic acid

* Author for correspondence: E-mail: tsocheva@polymer.bas.bg

1388–6150/2004/ $ 20.00

Akadémiai Kiadó, Budapest
Kluwer Academic Publishers, Dordrecht

(DBSA) as a surfactant and a counter-anion [9–11] allowed PANI to be blended homogeneously in a matrix of thermoplastic polymers. The long alkyl chains of the dodecylbenzene functional group act to make PANI compatible with bulk polymers with similar molecular structures (e.g. polyolefins) [9, 12, 13].

On the other hand, ultrahigh molecular mass polyethylene (UHMMPE) has unique and unmatchable physical and mechanical properties. UHMMPE has been regarded as an intractable polymer for which conventional melt processing is not possible. In addition, static charging in the UHMMPE products hampers its application. Instead, application of UHMMPE typically involves processing routes which strongly rely on full recovery of interfaces. UHMMPE has been the material of choice for use as a bearing material in total joint replacements for some time. The long relaxation time of UHMMPE chains provide a structural foundation for superior toughness and resistance to creep and wear [14].

Blends of UHMMPE and PANI have a great technological potential due to the remarkable properties of both polymers. It was shown previously [15] that composites of UHMMPE and PANI doped with DBSA (UHMMPE/PANI·DBSA) are conductive ($\sim 10^{-3}$–10^{-4} S cm^{-1}) at a content of PANI as low as 1 mass% and could be processed by the specific for UHMMPE techniques, such as hot pressing and powder sintering [16].

Valenciano *et al.* [17] deal with polymer blends of PANI protonated with camphorsulfonic acid and UHMMPE prepared by using the 'solution' method from a *m*-cresol/decaline mixture. According to the authors, besides the solubilization of the two polymers, the solvent mixture also promotes specific interactions that lead to improvement in solubility and conductivity of the blend.

In another study, films of UHMMPE-PANI composite [18] have also been prepared in solution. It was found that an unusual interpenetrating network morphology is formed in the blend systems. Besides, it is well known that thermal analysis methods are very useful in studying PANI and its blends with conventional polymers (e.g. [19–22]).

In this paper, the changes of the crystalline morphology of UHMMPE with temperature and on adding PANI·DBSA complex are investigated. It was focused on the characterization of the supramolecular structure of UHMMPE/PANI·DBSA composite. Experiments were carried out for both the net powdered UHMMPE and composite including 5 mass% of PANI by using differential scanning calorimetry (DSC) and wide-angle X-ray diffraction (WAXD).

To the best of our knowledge, for the first time supramolecular structure and crystallinity parameters of such a composite were analyzed.

Experimental

Preparation of PANI·DBSA complex

Powdered PANI·DBSA complex was prepared by oxidative polymerization of aniline (ANI) (Fluka, reagent-grade) in presence of DBSA (Tokyo Kasei) in aqueous medium, using ammonium peroxydisulfate (APDS) (Fluka) as an oxidant, following

the procedure described previously [23]. DBSA is in two-fold excess according to its ratio in PANI·DBSA complex (1 basic mol ANI to 0.5 mol DBSA).

Preparation of UHMMPE/PANI·DBSA composite

The UHMMPE/PANI·DBSA composite was prepared in situ by adding equimolar amounts of DBSA, ANI and APDS into powdered UHMMPE ('Neftochim', Bulgaria, molar mass $5 \cdot 10^6$) followed by bulk polymerization of ANI at 2–5°C for 4 h and subsequent vacuum drying at 50°C. The content of the net PANI in the composite is 5% by the mass of UHMMPE/PANI blend.

DSC

Thermal studies of UHMMPE, PANI·DBSA complex and their composite were performed on a Perkin Elmer DSC 7 differential scanning calorimeter using argon as a purge gas. The mass of the samples was ca. 6 mg. The instrument was calibrated with an indium standard for temperature and heat change. An empty aluminum pan was used as reference. The DSC traces shown in Fig. 1 are presented as obtained (without normalization).

Calorimetric measurements were performed in two ways: (1) starting from room temperature, samples were directly heated up to 180°C at a constant heating rate of 10°C min^{-1} followed by cooling with the same rate and reheating the samples under the same conditions; (2) heating the PAN·DBSA complex and UHMMPE/PANI·DBSA composite up to gradually rising programmed temperature (120, 150, 170, 200, 220, 250, 270, 300, 330, 350, 400 and 450°C) with a heating rate of 10°C min^{-1} and quenching af-

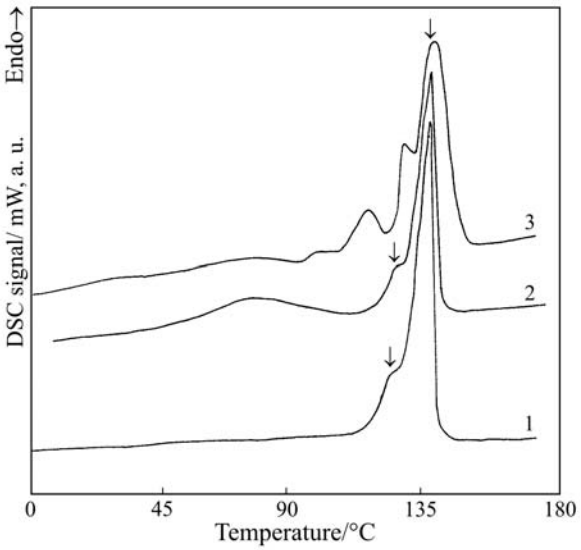

Fig. 1 DSC curves of 1 – net UHMMPE, 2 – UHMMPE/PANI·DBSA composite and 3 – PANI·DBSA complex registered upon direct heating up to 180°C at a heating rate of 10°C min^{-1}

ter each heating run in order to determine the experimental mass loss. It was calculated by weighing the sample pans prior to (W_{in}) and after (W_f) each heating run in the calorimetric chamber according to the equation:

$$\text{mass loss}\,(\%) = \frac{W_{in} - W_f}{W_{in}} 100$$

The crystallinity degree (X_C) of the samples was calculated (based on DSC traces) using the following formula:

$$X_c\,(\%) = \frac{\Delta H}{\Delta H_{100}} 100$$

where ΔH is the experimentally found heat of fusion of UHMMPE (net and in the composite) and ΔH_{100} is the heat of fusion of 100% crystalline polyethylene taken to be 289 J g^{-1} [24].

The ΔH of the UHMMPE crystals in the composite was calculated by the relationship:

$$\Delta H = \Delta H_{total} W$$

where ΔH_{total} is the sample enthalpy found by DSC and W is the mass fraction of UHMMPE in the sample (74.8 mass% UHMMPE in the composite, i.e. W=0.748).

WAXD

Philips APD 15 X-ray generator was used for the WAXD experiments. The point focus beam was monochromatized to CuK_α with a graphite crystal. The X-ray source utilized a CuK_α target (l_K=1.54178 Å) with generator settings of 40 kV and 30 mA. The 2θ step size for each individual data collection point was set to 0.025°.

Results and discussion

DSC traces, obtained upon the first direct heating the samples up to 180°C are presented in Fig. 1. Two groups of metastable crystallites of different size and perfection with melting temperature (T_m) of 129 and 144°C, respectively, are found in the net UHMMPE (curve 1) in accordance with the literature data [14, 25]. As seen in Table 1, presenting the thermodynamical DSC data, the melting temperature of the UHMMPE crystallites within the as-received composite with PANI·DBSA complex (curve 2) and of the net UHMMPE is almost the same. However, the ΔH of UHMMPE in the composite is approximately twice lower than the enthalpy of the net polymer. Thus, it can be suggested that the smaller UHMMPE crystallites have been destroyed during in situ polymerization of ANI, which results in a substantial drop of X_C of UHMMPE present in the composite. A broad endothermic peak (curve 2) in the temperature range from room temperature to approximately 110°C is observed and related to evaporation of water absorbed from the hygroscopic PANI·DBSA complex.

Table 1 Thermodynamical parameters obtained upon direct heating up to 180°C at a heating rate of 10°C min^{-1} of as-received samples

Sample	1st heating				2nd heating			
	T_m/°C	ΔH_{total}/J g^{-1}	ΔH/J g^{-1}	X_c/%	T_m/°C	ΔH_{total}/J g^{-1}	ΔH/J g^{-1}	X_c/%
UHMMPE	144.2		181.1	62.7	137.1		170.4	59.0
Composite	142.0	124.7	93.3	32.3	134.7	110.0	82.3	28.5

T_m – melting temperature; ΔH_{total} – heat of fusion of the sample; ΔH – heat of fusion of the UHMMPE; X_c – crystallinity degree

It was shown in our previous calorimetric study [26] that PANI·DBSA complex crystallizes during its preparation forming a variety of crystal phases (curve 3), evidenced by WAXD (Table 2). The large number of crystalline phases occurring in a broad temperature region (Fig. 1, curve 3) allows determination of the total heat of fusion of the complex (ca. 35 J g^{-1}) only. However, melting peaks of PANI·DBSA complex have not been observed for the UHMMPE/PANI·DBSA composite on its DSC heating trace (curve 2). We suppose this is due solely to the overlapping of the melting ranges of the constituents, since PANI·DBSA and UHMMPE cannot form mixed crystals. It is seen from Table 1, that ΔH_{total} is higher than ΔH found for the composite. Therefore, the PANI·DBSA complex forms its own crystals and the constituents in the composite studied are phase separated. The phase separation was confirmed by WAXD data that revealed, not unexpectedly, that the diffraction patterns of the UHMMPE/PANI·DBSA composite consisted simply of superimposed patterns of the pure components; there is no detectable indication of cocrystallization. WAXD data, i.e. interlayer Bragg spacings *d*,

Table 2 Interlayer Bragg spacings *d*(Å) estimated by WAXD

UHMMPE	UHMMPE/PANI·DBSA	PANI·DBSA
8.43	8.43	–
–	–	7.13
–	–	4.72
–	–	4.34
4.10	4.10	–
–	–	3.88
3.74	3.74	–
–	–	3.68
–	3.43	3.43
–	–	3.16
–	–	3.07
2.98	2.98	–
–	–	2.84
–	–	2.60
2.48	2.48	
–	2.42	2.42
2.28	2.28	–
2.22	2.22	–
2.18	2.17	–
2.11	2.11	–
1.94	1.94	–
1.73	1.73	–

are shown in Table 2. It can be assumed that PANI·DBSA complex has been distributed on the surface of UHMMPE particles resulting in an electrically conductive network.

It is well known that temperature is a very important parameter in processing of conducting polymers, since the thermal treatment affects the oxidation state and structure of the polymeric chains [27]. It has been suggested that temperature increase results in crosslinking of the polymers [28–30] (both alone and in the blends) and in removing of the counter anion, thus decreasing the conductivity. As mentioned in the Experimental, the DSC data for the mass loss of PANI·DBSA complex and UHMMPE/PANI·DBSA composite are obtained from DSC scanning runs recorded at gradually rising programmed temperature with a heating rate of 10°C min^{-1} followed by quenching after each heating run. The curves in Fig. 2 show that the PANI·DBSA complex, both net (curve 2) and in the UHMMPE matrix (curve 1) is thermally stable up to approximately 270°C, only absorbed water (up to 100°C) and free DBSA (up to 200°C) being removed. DBSA bounded electrostatically as a counterion has been evolved at higher temperature. Therefore, it can be supposed that the composite is processable without loosing conductivity at temperature much higher than T_m of UHMMPE.

It is known [31] that UHMMPE is a semicrystalline polymer having very long and entangled macromolecules able to crystallize in a wide variety of morphologies, in which the chain dimensions differ substantially. The UHMMPE melt crystallization results in a material of moderate crystallinity, the thickness of the crystalline lamellae being of the order of a few hundred angstroms. It was assumed that, upon melt crystallization, an individual chain can be incorporated into many different lamellae and amorphous regions, due to its very high molecular mass.

Using DSC data from Table 1, the average thickness of crystalline lamellae l_c was estimated from the melting temperature of the polymer via the Thomson–Gibbs equation [14]:

$$T_m = T_m^0 - T_m^0 \frac{2\sigma_c}{l_c \Delta H_{100}}$$

where T_m^0=145.55°C is the melting point for a hypothetical crystal of infinite size for which surface energy effects may be disregarded [25]. A value of $93 \cdot 10^{-7}$ J cm^{-2} was used for the fold surface energy, σ_e, which is related to the surface energy of the crystal end faces at which the chains fold. ΔH_{100} taken to be 289 J g^{-1} is equal to 289 J cm^{-3} (since the density of the crystalline phase is 1.000 g cm^{-3}) [32, 33].

The long period, L, which means the most probable next-neighbour distance of the lamellae, can be directly calculated from the data of l_c and X_C of the samples studied [34] using the relation $l_c = LX_c$. Then, the thickness of the amorphous phase l_a is obtained by $l_a = L - l_c$ [35]. The results are presented in Table 3.

According to the estimated crystallographic parameters, models of the crystalline morphology of net UHMMPE and UHMMPE/PANI·DBSA composite before and after melting and subsequent cooling (both at a rate of 10°C min^{-1}) are presented in Fig. 3. It is seen that the original structure of UHMMPE can not be completely re-

Table 3 Crystallographic parameters of UHMMPE estimated from the DSC results upon direct heating up to 180°C at a heating rate of 10°C min^{-1} of the samples

	1st heating			2nd heating		
	l_c/nm	L/nm	l_a/nm	l_c/nm	L/nm	l_a/nm
UHMMPE – net	69.4	110.8	41.4	11.1	18.9	7.8
UHMMPE – in the composite	26.4	82.0	55.6	8.6	30.4	21.8

l_c – average size of the crystalline lamellae; L – long period; l_a – average size of the amorphous phase

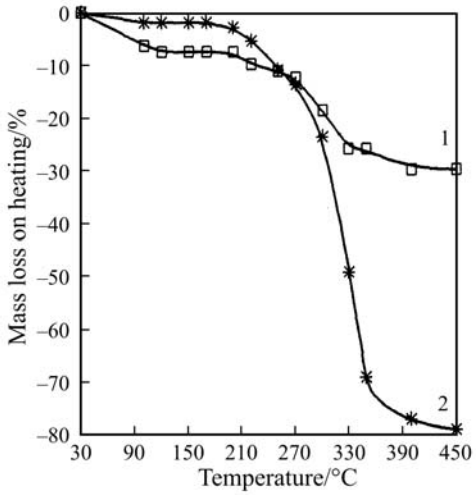

Fig. 2 Mass loss on heating up to gradually rising programmed temperature and subsequent quenching of 1 – UHMMPE/PANI·DBSA composite and 2 – PANI·DBSA complex *vs.* final heating temperature

covered after melting and relatively slow cooling. Since the crystallinity of melt recrystallized UHMMPE is only about 5% lower (Table 1) as compared to the original polymer it can be concluded that a large number of smaller crystals was obtained during the recrystallization evidenced by T_m drop (Table 1) and substantial decrease of L, l_c and l_a (Table 3).

The melting region and ΔH of UHMMPE and UHMMPE/PANI·DBSA composite were also determined during the heating up to gradually rising programmed temperature and subsequent quenching after each heating run. The crystallographic parameters were estimated from the DSC results as well. The data are presented in Table 4. The larger lamellae thickness corresponds to higher melting temperature, and vice versa. Calculated values for l_c were in the range from about 6 to about 23 nm depending on T_m.

It should be noticed that the final temperature of 120°C reached at the first heating is not high enough for UHMMPE melting. The polymer does not melt, but it undergoes

Table 4 Crystallographic parameters and T_m of UHMMPE obtained from the DSC results upon heating with a rate of 10°C min^{-1} up to gradually rising programmed temperature and subsequent quenching after each heating run

	Net UHMMPE					UHMMPE in the composite				
	l_c/nm	L/nm	l_a/nm	X_c/%	T_m/°C	l_c/nm	L/nm	l_a/nm	X_c/%	T_m/°C
to 150°C	22.6	34.6	12.0	65.4	141.4	23.1	67.4	44.3	34.3	141.5
to 170°C	6.9	16.0	9.1	43.0	132.0	7.1	29.9	22.8	23.8	132.4
to 200°C	7.8	17.0	9.2	45.7	133.5	6.1	26.5	20.4	23.0	130.2
to 220°C	6.8	15.4	8.6	43.8	131.7	6.1	25.7	19.6	23.7	130.2
to 250°C	6.8	15.8	9.0	43.1	131.8	6.5	26.5	20.0	24.4	131.1
to 270°C	6.5	15.0	8.5	43.5	131.2	6.0	23.9	18.0	24.9	129.8
to 300°C	6.6	14.6	8.0	45.4	131.4	5.5	20.6	15.1	26.8	128.6
to 330°C	7.2	15.0	7.8	48.4	132.6	5.1	16.9	11.8	30.3	127.3
to 350°C	7.2	12.9	5.7	55.4	132.5	5.1	13.1	8.0	39.0	127.3
to 400°C	6.4	12.6	6.2	50.5	130.8	5.2	12.4	7.3	41.6	127.4
to 450°C	6.0	9.2	3.2	65.3	129.9	5.7	13.1	7.4	43.2	129.1

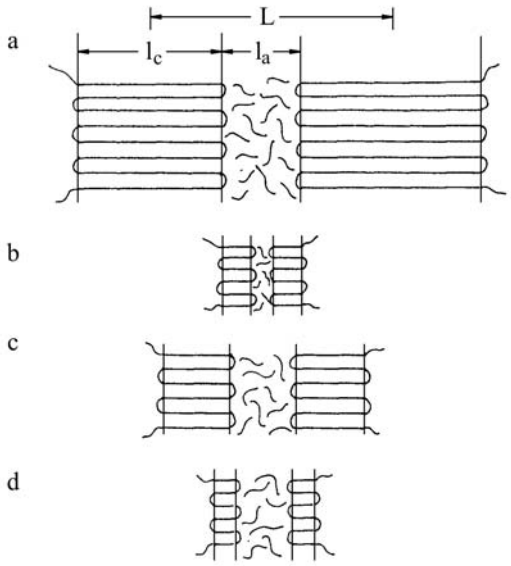

Fig. 3 Scheme of morphological changes in UHMMPE as a result of in situ polymerization of ANI and subsequent heating; a – net UHMMPE; b – net UHMMPE after melt crystallization; c – UHMMPE/PANI·DBSA; d – UHMMPE/PANI·DBSA after melt crystallization

structural changes. That is why the thermodynamical and crystallographic parameters obtained during the first melting, i.e. upon heating up to 150°C (Table 4), differ from those obtained upon first direct heating of as-received UHMMPE (Tables 1 and 3). L, l_c and l_a calculated for the preliminary heated up to 120°C UHMMPE (both net and in the composite) and subsequent quenching are substantially lower than those, calculated for the as-received polymer. T_m is lower as well. Therefore, lamellas of smaller size are formed upon the thermal treatment. The crystallographic parameters keep changing upon following heating up to gradually rising temperature. It is seen (Table 4) that the highest drop in the L, l_c and l_a appears upon the second melting (up to 170°C). Then the crystallographic parameters decrease regularly. The coincidence of l_c values for the net UHMMPE and UHMMPE presented in the composite (Table 4) is another evidence for the phase separation in the UHMMPE/PANI·DBSA composite. UHMMPE crystallizes regardless of the presence of PANI·DBSA complex. The values of L and l_a for UHMMPE in the composite, however, are much higher than these for the net polymer (Table 4). Hence, this fact shows unambiguously that PANI·DBSA complex is situated in the amorphous phase of the UHMMPE, forming its own crystalline and amorphous regions.

X_C data of the net UHMMPE given in Tables 1 and 4 are related to the as-received samples (Table 1) and samples subjected to preliminary heating up to 120°C and subsequent quenching (Table 4), respectively. As seen from Fig. 4, ΔH also depend substantially on the melting and crystallization conditions. It can be assumed that the crystalline structure of the net UHMMPE developed at higher temperature can not be fully

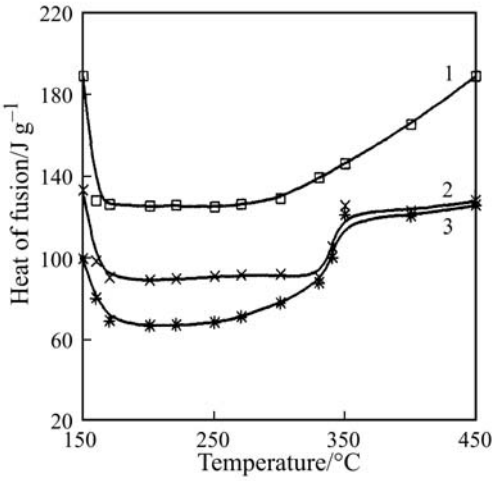

Fig. 4 Heat of fusion of 1 – net UHMMPE, 2 – UHMMPE/PANI·DBSA composite and 3 – UHMMPE in the composite registered upon heating up to gradually rising programmed temperature and subsequent quenching *vs.* final heating temperature

frozen by quenching. Both ΔH (Fig. 4, curve 1) and crystallographic parameters (Table 4) decrease abruptly upon each subsequent heating up to about 170°C. Then, the crystallinity and ΔH remain almost constant up to about 270°C but they start to grow up upon heating up to higher temperature. We assume that thinner lamellae of UHMMPE crystallites (T_m decreases) appeared in the amorphous region between pre-existing thick lamellae during the quenching process. They are thermally unstable being destroyed during the following heating and melting, respectively. However, the higher the final heating temperature, the greater the flexibility of UHMMPE macromolecular segments. Therefore, the mentioned above smaller crystallites appear again upon the next fast cooling in a greater amount, resulting in increased ΔH at temperatures higher than 270°C. It is seen that ΔH almost reaches its original value upon heating up to 450°C (Fig. 4, curve 1).

When UHMMPE is in composite with PANI·DBSA its crystallization behavior is almost the same (Fig. 4, curve 3). However, a great jump in the crystallinity upon heating at about 330°C is observed both for the UHMMPE and for the composite as a whole (Fig. 4, curve 2). ΔH_{total} for the composite is greater than for the matrix polymer up to about 330°C. Then they are overlapping. It is another evidence that PANI·DBSA forms its own crystals until the evolution of electrostatically bound as a counterion DBSA (Fig. 2, curve 1). Above this temperature PANI itself can not crystallize and ΔH_{total} and ΔH become equal.

Conclusions

It was found that during in situ preparation of PANI·DBSA complex in powdered UHMMPE, the crystalline phase of the matrix polymer has been partially destroyed

forming smaller crystallites. The complex has been distributed on the UHMMPE particles, resulting in an electrically conductive network. The average size of the amorphous regions of UHMMPE in the composite remains constant and does not change during the second direct heating, in contrast to the net polymer. It can be supposed that, during the melting of the UHMMPE crystals, PANI partially penetrates in the amorphous phase of the matrix polymer due to the presence of DBSA acting as a surfactant and compatibilizing UHMMPE and PANI molecules.

DSC results show that the composite studied is thermally stable up to approximately 270°C. Therefore, it can be supposed that UHMMPE/PANI·DBSA composite can be processed without loosing conductivity at temperature higher than T_m of UHMMPE.

* * *

The authors appreciate the financial support provided by the Bulgarian Ministry of Education and Science, contract X-905. They thank S. Vassilev for performing the X-ray diffraction measurements.

References

1 T. Kobayashi, H. Yoneyama and H. Tamura, J. Electroanal. Chem., 161 (1984) 419.
2 G. Gustafsson, Y. Cao, G. M. Treacy, N. Colaneri and A. J. Heeger, Nature, 354 (1992) 477.
3 K. Tzou and R. V. Gregory, Synth. Met., 53 (1993) 365.
4 B. Z. Tang, Y. Geng, J. W. Y. Lam, B. Li, X. Jing, X. Wang, F. Wang, A. B. Pakhomov and X. X. Zhang, Chem. Mater., 11 (1999) 1581.
5 H. K. Lin and S. A. Chen, Macromolecules, 33 (2000) 8117.
6 S. A. Chen and G. W. Hwang, J. Am. Chem. Soc., 117 (1995) 10055.
7 S.-J. Su and N. Kuramoto, Synth. Met., 108 (2000) 121.
8 Y. Haba, E. Segal, M. Nakis, G. I. Titelman and A. Siegmann, Synth. Met., 110 (2000) 189.
9 Y. Cao, P. Smith and A. J. Heeger, Synth. Met., 48 (1992) 91.
10 C. Y. Yang, P. Smith, A. J. Heeger, Y. Cao, J.-E. Oesterholm, Polymer, 35 (1994) 1142.
11 W.-Y. Zheng, R.-H. Wang, K. Levon, Z. Y. Rong, T. Taka and W. Pan, Macromol. Chem. Phys., 196 (1995) 2443.
12 J. Yang, C. Zhao, D. Cui, J. Hou, M. Wan and M. Xu, J. Appl. Polym. Sci., 56 (1995) 831.
13 Ch.-F. Liu, T. Maruyama and T. Yamamoto, Polym. J., 25 (1993) 363.
14 S. Andjelic and R. E. Richard, Macromolecules, 34 (2001) 896.
15 L. Terlemezyan, M. Radenkov, P. Mokreva, Ph. Radenkov and A. Atanassov, J. Polym. Mater., 20 (2003) 213.
16 R. D. Hanna, Encyclopedia of Polymer Science and Engineering, Wiley, New York 1986, p. 493.
17 G. R. Valenciano, A. E. Job and L. H. C. Mattoso, Polymer, 41 (2000) 4757.
18 A. Andreatta and P. Smith, Synth. Met., 55 (1993) 1017.
19 H. Yan, N. Sada and N. Toshima, J. Therm. Anal. Cal., 69 (2002) 881.
20 K. Pielichowski, J. Therm. Anal. Cal., 54 (1998) 171.
21 J. Pielichowski, J. Therm. Anal. Cal., 53 (1998) 633.
22 R. F. de Farias and L. M. Nunes, J. Therm. Anal. Cal., 70 (2002) 559.
23 N. Gospodinova, P. Mokreva, T. Tsanov and L. Terlemezyan, Polymer, 38 (1997) 743.

24 B. Wunderlich and C. M. Cormier, J. Polym. Sci. A-2, 1967, 5, 987.
25 G. W. H. Hohne, Polymer, 43 (2002) 4689.
26 D. Tsocheva, T. Tsanov, L. Terlemezyan and S. Vassilev, J. Therm. Anal. Cal., 63 (2001) 133.
27 A. Boyle, J. F. Penneau, E. Genies and C. Riekel, J. Polym. Sci., Part B, 30 (1992) 265.
28 J. E. Pereira da Silva, D. L. A. de Faria, S. I. Cordoba de Torresi and M. L. A. Temperini, Macromolecules, 33 (2000) 3077.
29 J. E. Pereira da Silva, S. I. Cordoba de Torresi, D. L. A. de Faria and M. L. A. Temperini, Synth. Met., 101 (1999) 834.
30 D. Tsocheva, T. Zlatkov and L. Terlemezyan, J. Therm. Anal. Cal., 53 (1998) 895.
31 Y.-Q. Xue, T. A. Tervoort and P. J. Lemstra, Macromolecules, 31 (1998) 3075.
32 O. Darras and R. Seguela, Polymer, 34 (1993) 2946.
33 N. Okui, N. Narita, T. Shimada and T. Kawai, Koubunshi Ronbunshuu, 31 (1974) 469.
34 L. Hubert, L. David, R. Seguela, G. Vigier, C. Degoulet and Y. Germain, Polymer, 42 (2001) 8425.
35 J. Y. Nam, Sh. Kadomatsu, H. Saito and T. Inoue, Polymer, 43 (2002) 2101.